We are IntechOpen,
the world's leading publisher of Open Access books
Built by scientists, for scientists

6,900
Open access books available

186,000
International authors and editors

200M
Downloads

154
Countries delivered to

Our authors are among the

TOP 1%
most cited scientists

12.2%
Contributors from top 500 universities

BOOK CITATION INDEX
CLARIVATE ANALYTICS
INDEXED

WEB OF SCIENCE™

Selection of our books indexed in the Book Citation Index
in Web of Science™ Core Collection (BKCI)

Interested in publishing with us?
Contact book.department@intechopen.com

Numbers displayed above are based on latest data collected.
For more information visit www.intechopen.com

Chapter

Advanced Biosensing towards Real-Time Imaging of Protein Secretion from Single Cells

Lang Zhou, Pengyu Chen and Aleksandr Simonian

Abstract

Protein secretion of cells plays a vital role in intercellular communication. The abnormality and dysfunction of cellular protein secretion are associated with various physiological disorders, such as malignant proliferation of cells, aberrant immune function, and bone marrow failure. The heterogeneity of protein secretion exists not only between varying populations of cells, but also in the same phenotype of cells. Therefore, characterization of protein secretion from single cell contributes not only to the understanding of intercellular communication in immune effector, carcinogenesis and metastasis, but also to the development and improvement of diagnosis and therapy of relative diseases. In spite of abundant highly sensitive methods that have been developed for the detection of secreted proteins, majority of them fall short in providing sufficient spatial and temporal resolution for comprehensive profiling of protein secretion from single cells. The real-time imaging techniques allow rapid acquisition and manipulation of analyte information on a 2D plane, providing high spatiotemporal resolution. Here, we summarize recent advances in real-time imaging of secretory proteins from single cell, including label-free and labelling techniques, shedding light on the development of simple yet powerful methodology for real-time imaging of single-cell protein secretion.

Keywords: cytokines, growth factors, SPR imaging, nanoplasmonic, interferometric scattering microscopy, Photonic Crystal Resonator, fluorescence, total internal reflection fluorescence

1. Introduction

Cells secrete proteins into the extracellular environment to achieve important physiological processes, such as transportation of nutrients, digestion of food, regulation of metabolic processes, etc [1–5]. Cell secretion can be classified into the constitutive and regulated secretory pathway [6–8]. The constitutive secretory pathway is associated with transportation of secretory vesicles to the cell surface and their release independently of stimulus [9–11]. The regulated secretory pathway produces secretory granules, stores them in the cytoplasm, and secretes them into the extracellular environment only upon receiving stimuli [12]. In human, more than 15% of the genome encoded proteins are associated with the secretion process [13]. These released proteins include neurotransmitters, protein hormones,

growth factors, cytokines, enzymes, antibodies, etc [14]. They play a vital role in intercellular communication [15], which further regulates cell functions in immunology [16–18], neurobiology [19–21], endocrinology [22–24], etc. For instance, as the immune cells are stimulated, they undergo dynamic alternation and secrete various types of cytokines in a heterogenous manner. These secreted cytokines regulate the maturation and growth of immune cells, and activate the immune effector and memory immune responses.

The heterogeneity of cellular protein secretion has been found in various human diseases, including malignant proliferation of cells, aberrant immune function, bone marrow failure, etc [25–27]. This heterogeneity is present between distinct cell populations such as normal and pathological cells, as well as the same phenotype of cells [28–30]. This secretome heterogeneity creates diverse microenvironment for cells. The proliferation and metastasis of tumor cells can be prohibited or promoted upon the discrepancy of microenvironment, in spite of within the same tumor [31]. Meanwhile, the secretome change is frequently associated with atypical cellular phenotypes [32], which are indicative of diseases such as cancers, thus can be used as significant markers for tumorigenic process at single cell level. Therefore, characterization of protein secretion from single cell play a vital role in not only understanding the intercellular communication in immune effector, carcinogenesis and metastasis, but also developing and improving the current diagnosis and therapy of relative diseases [33–35]. In spite of abundant highly sensitive methods that have been developed for the detection of secreted proteins, majority of them have insufficient resolution in space and time, thus are not capable of providing deep insight into the behavior of protein secretion from single cells. Ideally, a detection method is supposed to be equipped with a high spatial resolution that enables differentiation of single cells from each other, and visualization of the spatial distribution of secreted proteins among multiple single cells, as well as a high temporal resolution that can recognize the dynamic alteration of secretion in a quantitative manner. The real-time imaging techniques feature rapid acquisition of analyte information on a 2D plane, and high spatial and temporal resolution, thus attract considerable attention in recent years, for its high potential to realize the deep exploration of single cellular protein secretion. Here, we review the involved works towards real-time imaging of single cell's protein secretion, including the detection of single or multiplex protein secretion, from group cells or single cells, in a real-time or near real-time manner, analyze their advantages and limitations, and discuss their major challenges.

2. Label-free techniques

In previous works, the real-time monitoring of cell secretion was achieved by label-free techniques such as plasmonic sensors, or label-required techniques such as fluorescence microscopy. The principles for all these methods are demonstrated in **Figure 1**. The representative works are summarized as shown in **Table 1**.

2.1 Plasmonic sensors

Plasmonic sensors have received tremendous attention owing to the label-free process, high sensitivity and fast response [36–38]. Plasmonic sensors generate surface plasmons and evanescence field that is sensitive to the changes of refractive index on sensing interfaces [39, 40]. By functionalization of the sensing interfaces, the change of refractive index upon specific binding of target molecules can be recognized. The plasmonic sensing could be implemented on varying materials, geometries and structures, such as flat metal films (surface plasmon resonance)
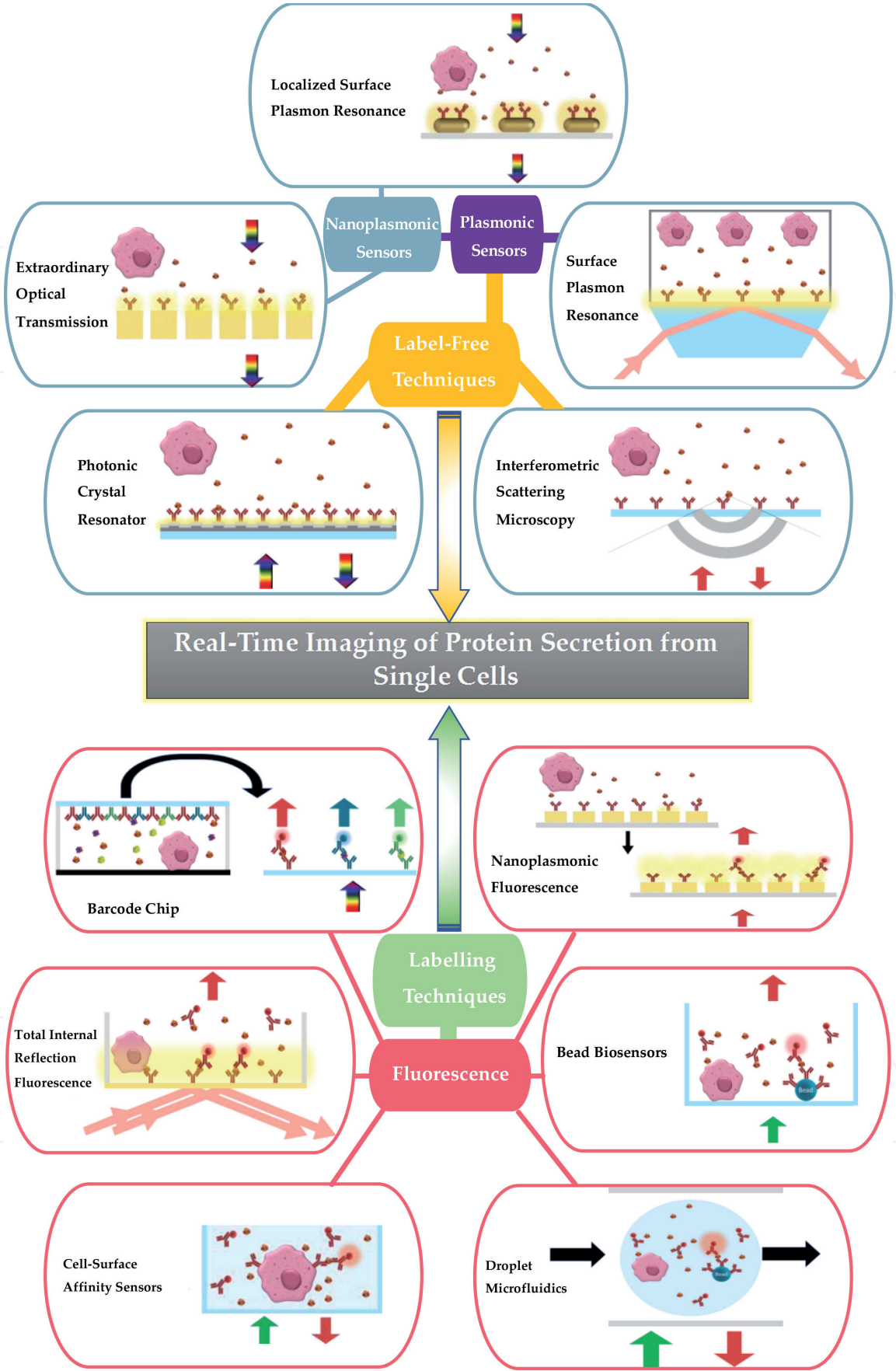
Figure 1.
Demonstration of methodology towards the real-time imaging of protein secretion from single cells.

[41, 42], nanoparticles (localized surface plasmon resonance) [43, 44] and nanoholes (extraordinary optical transmission) [45, 46]. These differences result in diverse applications and sensor performances.

Detection method	Cell	Stimuli	Secretion molecule	Cell confinement	Surface functionalization	Multiplex detection	Real-time imaging	LOD	Ref.
SPR	Human ovarian carcinoma SKOV-3	Ca^{2+} ionophore	VEGF	Attached on the ceiling of a flow cell chamber by gelatin	Gold/MUA/protein G/antibody	No	No	<100 ng/mL	[48]
SPR imaging	Murine B cell hybridoma	No	HEL-specific antibodies	Suspended in medium for sedimentation	Gold/electro-copolymerization of pyrrole and pyrrole-modified antigen	No	Yes (for group cells)	<50 ng/mL	[49]
SPR imaging	Human CD4+T-cells	TB-specific proteins, ESAT-6, CFP-10	IFN-γ	Captured on poly(OEGMA-co-HEMA) / anti-CD4+ antibody	Poly(OEGMA-co-HEMA) brush/ antibody	No	Yes (for group cells)	50 ng/mL	[50]
SPR imaging	EpCAM hybridoma	No	Anti-EpCAM antibodies	Suspended in medium for sedimentation	Gold/hydrogel/ EpCAM	No	Yes (for single cells)	N.A.	[51]
LSPR	Jurkat T cells	No	IL-6	Enclosed in a microwell	Gold-capped nanopillar-structured cyclo-olefin-polymer film/ MUA/antibody	No	No	10 ng/mL	[62]
LSPR	Jurkat T cells	Ionomycine, phorbol myristal acetate (PMA)	IL-2, IL-10, IFN-γ, TNF-α	Separate operation for cell secretion and detection	CTAB-coated AuNRs/ /MUA/ antibodies	Yes	No	20−30 pg/mL	[63]
LSPR	Jurkat T cells	Oligomeric and amyloid fibrils	IL-6 ,TNF	Separate operation for cell secretion and detection	CTAB-coated AuNRs/ /MUA/ antibodies	Yes	No	N.A.	[64]

Detection method	Cell	Stimuli	Secretion molecule	Cell confinement	Surface functionalization	Multiplex detection	Real-time imaging	LOD	Ref.
LSPR	Neutrophils	PMA	Fibrils, neutrophil extracellular traps	Enclosed in a microwell	Gold-capped nanopillar-structured cyclo-olefin polymer	No	No	N.A.	[65]
LSPR	9E10 Hybridoma cells	No	Anti-c-myc antibodies	Suspended in medium for sedimentation	Au nanostructure/c-myc peptide	No	Yes (for single cell)	100 pM (~4.88 ng/mL)	[66]
Extraordinary Optical Transmission	Hela cells	Ca^{2+} ionophore A23187	VEGF	Cells grow in a cell module, the secreted cytokines are delivered to the adjacent detection module.	Gold nanohole/PEG-ylated Alkanethiol/streptavidin/biotinylated antibodies	No	No	145 pg/mL	[68]
Extraordinary Optical Transmission	EL4 lymphoma cells	Ionomycin and PMA	IL-2	Enclosed in a small-volume microchamb-er with valve gates and hydraulic regulat-ion channel	Gold nanohole/PEGylated alkanethiols/streptavidin/biotinylated antibody	No	Yes (for single cell)	39 pg/mL	[69]
Photonic crystal resonant	HepG2 liver cells, baby hamster kidney cells	No	Thrombopoietin	Suspended in medium for sedimentation	Si_3N_4/oxidized dextran/antibodies	No	Yes (for single cell)	<125 ng/mL	[72]
Interferometric scattering	Epstein−Barr virus-transformed B cell line, Laz 388	No	IgG antibodies	Suspended in medium for sedimentation	NHS coated glass/anti-IgG antibodies	Yes	Yes (for single cell)	N.A.	[75]

Detection method	Cell	Stimuli	Secretion molecule	Cell confinement	Surface functionalization	Multiplex detection	Real-time imaging	LOD	Ref.
Microengraving	Human peripheral blood mononuclear cells	B cell receptor crosslinking antibody and CD40L	IFN-γ, IL-6, proinsulin-reactive antibodies	Enclosed in a microwell	Epoxy coated glass slide/ antibodies or antigens	Yes	No	N.A.	[79]
Barcode chip	U937-derived macrophages	Lipopolysaccharide	42 types of immune effector proteins	Enclosed in a microwell	Glass slide/ poly-L-lysine/ antibodies	Yes	No	N.A.	[81]
Total Internal Reflection Fluorescence	Human peripheral blood CD14$^+$ monocytes	Lipopolysaccharide, ATP	IL-6, IL-1b	Enclosed in a microwell	Aminated glass slide/ antibodies	No	Yes (for single cell)	2000 molecules	[82]
Nanoplasmonic resonator	Jurkat T cells	Ionomycin and PMA	IL-2	Suspended in medium for sedimentation	Gold nanostructure array/ poly-D-lysine/ antibody	No	Yes (for single cell)	<100 ng/mL	[83]
Bead	Human peripheral blood CD4$^+$ T cells	Ionomycin and PMA	IFN-γ	Enclosed in a microwell	Streptavidin-coated microbeads/ biotinylated antibodies	No	No	21.4 ng/mL	[86]
Bead	Human peripheral blood CD56^{dim}CD16$^+$ NK cells	Ionomycin and PMA	IFN-γ	Enclosed in a microwell	Anti- IgG-Fc beads/ antibodies	No	No	2.5 ng/ml	[87]
Bead	Human peripheral blood mononuclear cells	Phytohaemagglutinin	IL-6, IL-8, TNF	Cells grow in a culture chamber, the secreted cytokines are delivered a the adjacent detection unit.	Commercial bead detection kit	Yes	No	20 pg/ml	[88]

Detection method	Cell	Stimuli	Secretion molecule	Cell confinement	Surface functionalization	Multiplex detection	Real-time imaging	LOD	Ref.
Cell-surface affinity	BV2 microglial cells	Lipopolysaccharide	IL-6	Suspended in medium for sedimentation	Biotinylated cell surface/neutravidin/ biotinylated antibody	No	No	0.1 pg/ml	[96]
Droplet microfluidics	Human peripheral blood mononuclear T cells	Ionomycin and PMA	IFN-γ	Encapsulated in a droplet	Cell surface/ cholesterol/aptamer	No	No	14.5 ng/mL	[94]
Droplet microfluidics	Jurkat T cells	Ionomycin and PMA	IL-2, IFN-γ, TNF-α	Encapsulated in a droplet	Commercial bead detection kit	Yes	No	N.A.	[99]
Droplet microfluidics +LSPR	MDA-MB-213 breast cancer cells, HL-60 leukemia cells	TNF-α	VEGF, IL-8	Encapsulated in a droplet	Gold nanorod/ PEGylated alkanethiols/ antibody	Yes	No	6–7 ng/mL	[100]

N.A., not applicable; MUA, 11-Mercaptoundecanoic acid or 10-carboxy-1-decanethiol; AuNR, gold nanoparticle.

Table 1.
Summery for detection methodology of real-time monitoring of cell secretion.

2.1.1 Surface plasmon resonance (SPR)

SPR is a sensitive label-free technique for characterization of molecular interaction and detection of molecules through the affinity recognition. Due to surface plasmons excited on the surface of a thin metal film and an evanescence field created on surface, the refractive index change in the vicinity of the sensor surface (within ~200 nm) can be detected. This relatively large sensing depth allows SPR to monitor the changes occurred not only on surfaces, but also in the bulk. SPR has been applied in various studies for molecules with molecular weight between 1000 Da~500 kDa [47]. Liu et al. [48] attached human ovarian carcinoma SKOV-3 cells on the ceiling of a flow cell chamber, and detected their vascular endothelial growth factor (VEGF) secretion by monitoring the SPR signal of the antibodies-immobilized gold chip at the bottom of the flow cell. This SPR sensor has a linear dynamic range of 0.1–2.5 μg mL^{-1}. Of note, even though SPR features label-free measurement and high sensitivity, the lack of spatial resolution restricts its application in the mapping of protein secretion. In the meantime, SPR imaging is suitable to achieve this goal. Instead of measurement of the SPR angle shifts in SPR spectroscopy, plenty of SPR imaging systems use fixed angle and wavelength of incident light for the excitation of SPR so that the reflection intensities of multiple spots within imaging area are obtained simultaneous.

Milgram et al. [49] took advantage of SPR imaging to real-time monitor the secretion of immunoglobulins from B-cells hybridoma. They assembled an antigen microarray using electro-copolymerization of free pyrrole and pyrrole-modified antigen on a gold chip. The secreted immunoglobulins were captured by the antigen proteins, triggering the refractive index changes. The SPR intensity changes were consequently observed at a fixed angle using a 12-bit CCD. A sharp SPR kinetic curve was observed after several minutes of incubation, indicating fast and sensitive detection of immunoglobulins. Wu et al. [50] used anti-CD4 antibody to capture and immobilize human CD4$^+$T-cells on a sensing chip, and detected their in-situ secretion of Interferon gamma (IFN-γ) through functionalized anti-IFN-γ antibody located at the neighboring sites. The detection limit for IFN-γ was ~50 ng/mL. Stojanović et al. [51] applied SPR imaging to quantify the antibody production from single EpCAM hybridoma cells. Based on the measured SPR signal alteration, the overall secretion antibody amount from a single cell was calculated as 0.02 to 1.19 pg per cell per hour. However, this estimation is questionable because not all the antibodies secreted from cell were captured. To solve this problem, they performed simulation using COMSOL Multiphysics and found the captured antibodies by sensors accounts for 99% of the excreted antibodies, only 1% excreted antibodies are not detected [52].

A major limitation of intensity-based SPR imaging is its relatively low sensitivity. Compared to SPR of high sensitivity, intensity-based SPR imaging suffers from one order of magnitude lower of sensitivity [53]. This relatively low sensitivity is dominantly contributed by the fluctuations of the incident light intensity, photon statistics associated shot noise, and detector noise [54]. This issue could be improved by performing optical multilayer structured long-rang surface plasmons [55], angle-resolved or spectral SPR imaging [56], NIR light source [57], etc.

2.1.2 Nanoplasmonic biosensors

Different from SPR sensors utilizing propagating surface plasmons generated on flat metal film, nanoplasmonic sensors generate and manipulate localized surface plasmons on nanostructures [58]. Conventionally, nanoapertures or nanoparticles are fabricated to interact with light, leading to localized surface plasmon resonance

(LSPR) or extraordinary optical transmission (EOT). As nanoplasmonic biosensors combine with cell imaging, a powerful tool is created for protein secretion imaging. Nanoplasmonic biosensors generate strong evanescence field in the vicinity of less than 30 nm, thus are highly sensitive to the local refractive index changes, allowing the detection of target molecules captured on surfaces. Since the excitation of these nanostructures did not require complex optical devices, the instrumentation can be simple and straightforward. By tracing the dynamic alteration of reflection or transmission spectra, these changes can be recorded in a simple and real-time manner. Therefore, this feature allows a simple-but-sensitive label-free detection.

2.1.2.1 Localized surface plasmon resonance (LSRP)

LSRP generated on nanostructures results in the collective oscillation of electrons at the interface of metallic structures. A localized electromagnetic field is sensitive to the nanostructure shape and changes of refractive index at the distance of 10–30 nm [59, 60]. A molecular binding event on these nanostructures, causes a red shift in SPR peak, and gives rise to the scattering intensity of light at the same time. Due to a short electromagnetic field decay length, LSPR is insensitive to the changes of the refractive index in bulk, therefore the bulk effect can be minimized. This feature allows LSPR to measure temperature-dependent binding process, and investigate the effects of various environment factors on molecular interactions, such as solution pH and ionic strength [61].

LSPR measurement can be implemented by recording either SPR peak shift or scattering intensity changes. In the SPR peak shift based detection, Zhu et al. [62] combined microwell technique with LSPR to monitor Interleukin 6 (IL-6) secretion in the single cell level. The microwells were adapted to trap cells, a gold-capped nanopillar-structured cyclo-olefin-polymer film was covered on the top of microwells. The transmittance spectrum of the gold nanostructured surface provides real-time information on the absorption peak shift of nanogold during cell secretion. This nanostructured film further fabricated with Anti-IL-6 antibody realized a detection limitation of 10 ng/mL for IL-6.

In the scattering intensity based detection, Oh et al. [63] developed a multiplexed LSPR system for simultaneous measurements of pro-inflammatory cytokines (IL-2, IFN-γ, and TNF-α) and anti-inflammatory cytokines (IL-10) secreted by T cells. The cell culture and cytokine detection were conducted in independent steps. The sensitivity reached 20−30 pg/mL. Faridi et al. [64] applied similar system to characterize the secretion of IL-6 and tumor necrosis factor alpha (TNF), secreted from human monocytes and lymphocytes. The same principle has been applied to monitor neutrophil extracellular traps (NETs) and fibril released from single neutrophils [65]. Raphael et al. [66] achieved the real-time imaging of anti-c-myc antibodies secreted from single hybridoma cells with gold nanostructured arrays. The electron beam lithography was implemented to fabricate the square arrays of gold nanostructure on glass coverslips. The gold nanostructure arrays have a diameter of 70 nm, a height of 75 nm and a separation distance of 300 nm. The differing distances between the position of the settled single cell and the centers of arrays provide spatial resolution to observe the protein secretion. The c-myc peptides conjugated to plasmonic gold nanostructures captured the secreted anti-c-myc antibodies in a real-time manner. The caused binding displayed an increase in scattering intensity due to LSPR effect, which is measured through changes of light reflection. In parallel with reflected light based LSPR characterization, the transmitted light and fluorescence microscopy were integrated for live cell imaging. The transmitted light imaging enables observation of the position of single cell and its morphological change. The fluorescence microscopy allows

the monitoring of membrane dynamics through a cell plasma membrane label-dye rhodamine DHPE, which distinguishes the signal due to occasional outward protrusions of lamellipodia from protein secretion signal. To model the singular cell secretion, the cell was assumed a spherical emitter producing a propagating pulse of antibodies with a Gaussian concentration profile, where the diffusion constant $D = r^2/6 \cdot t$. This method provides a sensitivity of 100 pM (~4.88 ng/mL) for the detection of anti-c-myc antibodies.

2.1.2.2 Extraordinary optical transmission (EOT)

In EOT biosensor, regularly periodic nanohole structure of subwavelength in a metallic film results in significant enhancement of light transmission through the nanoholes. This phenomenon is associated with both localized and propagating surface plasmons on the nanohole structures. By collecting and analyzing the transmission spectra, the light frequency-dependent transmission enhancement could be easily recognized. The molecular binding event on surface is corresponding to the transmission spectral shift. Consequently, the binding event can be visualized in a real-time manner through tracking the changes of transmission spectra. Combining localized and propagating surface plasmons, the spectra of EOT provide a wealth of information with varying sensitivities at different regions of nanoholes. In addition, the nanohole structures allows the flow-through design, which changes the manner of the mass transfer of analytes, and increases delivering rate of analytes from bulk to the sensing surface [67].

To achieve real-time imaging of cell secretion, Li et al. [68] first developed a microfluidic device that separated a cell culture module and an EOT sensing module. The nanohole array sensor has a hole diameter of 200 nm and a periodicity of 600 nm, and was fabricated by deep-UV lithography and functionalized by biotinylated antibodies. This detection module is directly connected with an adjacent cell culture module made of a zigzag single-channel PDMS unit. This biosensor system achieved a detection limit of 145 pg/mL for VEGF. In this study, the VEGF secretion was detected from the media containing a group of cancer cells, and the mapping of secretion was disabled due to the separated configuration of detection and cell culture modules. Subsequently, they developed a microfluidic system suitable for the secretion imaging of a single cell [69]. Enclosed in a microchamber, a single cell was attached to nanohole arrays, functionalized by antibodies. To achieve the function of real-time imaging, spectrum profiles on a perpendicular 1D line was collected, and the selected positions of the region-of-interest were analyzed. This sensor achieved a detection limit of 39 pg/mL for interleukin-2 (IL-2) in complex media.

2.2 Photonic Crystal Resonator (PCR)

Similar with plasmonic sensors, Photonic Crystal Resonator (PCR) exploits an evanescence field to interact with and sense the surrounding medium, i.e. the changes of its refractive index. PCR is created by Photonic Crystals (PCs) that own periodically varied refractive indices, which forbid the light propagation of certain wavelength of light in certain directions inside the material. This causes constructive or destructive interference of the light, and therefore a minimum in the transmission spectrum and a maximum in the reflection spectrum could be observed. Dependent on material, geometry and the index contrast, the decay length of PCs ranges from dozens of nanometers to the order of a few microns [70]. PCs composed of silicon nitride (Si_3N_4) or titanium dioxide (TiO_2) have been proved able to achieve cellular imaging with resolution 2–6 μm [71].

Juan-Colás et al. [72] monitored the secretion of thrombopoietin at single cell level using photonic crystal resonant imaging (**Figure 2**). The PCR surface microfabricated by electron beam lithography, consists of a grating with period of 555 nm on a 150-nm-thick Si_3N_4 film. It displayed a penetration depth of ~200 nm. To realize hyperspectral resonance image, reflection spectra was taken in a sequence of illumination wavelengths with 0.25-nm wavelength step. Under each wavelength, the intensity value of each pixel was analyzed and fit into a Fano resonance curve to accurately obtain the resonance wavelength for each pixel. To create a sensitive surface for analyte capture, antibodies were functionalized on a 3D matrix consisting of branched glucan dextran, which increased the density of antibodies on the surface. This sensor was demonstrated to detect lower than 125 ng/mL of suspended recombinant Human thrombopoietin. The interaction of antibody-antigen was treated as a single adsorption process, and the protein secretion was modeled as a Langmuir adsorption distribution. By quantifying the total secretion area in a timely manner, the single-cell secretion rate was calculated as 22 µm2/h. In addition, the wide field of view allows parallel imaging of 30 cells on an area of 500 × 500 µm, so that their dynamics and the kinetics could be characterized simultaneously.
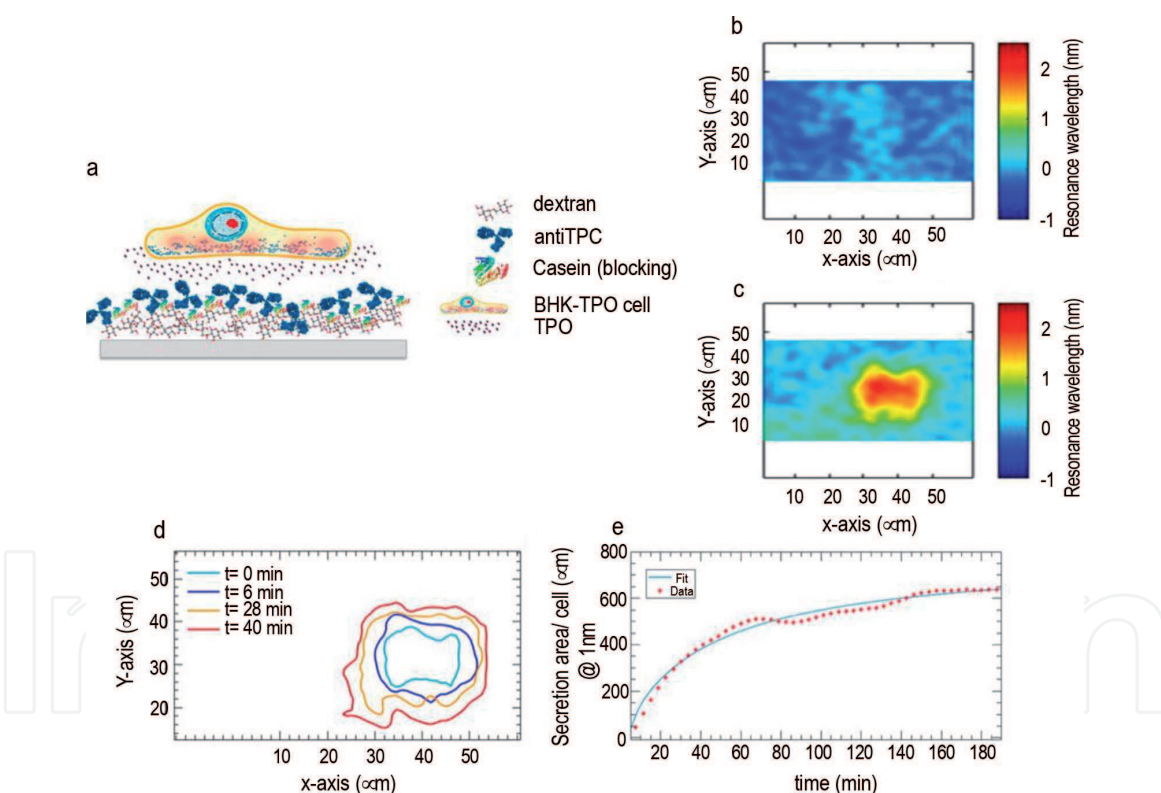

Figure 2.
Photonic crystal resonant imaging protocol for monitoring TPO secretion from a single BHK-TPO cell. (a) Dextran molecules are employed to create a 3D network of antibodies. Casein protein is employed as a blocking agent to prevent nonspecific binding from other proteins expressed by the cells. The secreted cytokines (i.e., TPO) from attached cells diffuse through the 3D network to specifically bind to the antibodies immobilized throughout the dextran network. The amount of deposited casein protein is optimized to maximize the signal-to-noise ratio of the detection system. (b) The region of interest (55 × 40 µm), with a wavelength uniformity of Δλ ± 0.5 nm. (c) A hyperspectral PCRS image reveals the adhesion of a -BHK-TPO cell to the PCRS, whose high concentration of cell adhesion molecules located in the inner region is translated into a higher refractive index content area. (d) Over time, this secretion area increases as TPO molecules are secreted from the cell and bind to the surface-immobilized antibodies, therefore locally increasing the refractive index around the BHK- TPO area. (e) The secretion of TPO is then monitored over time, and a Langmuir adsorption distribution is fitted to the data to model the secretion from the BHK-TPO cell accounting for the area covered by the adhered cell. Reprint (adapted) with permission from Ref. [27] under the terms of the Creative Commons Attribution License. Copyright 2018 Juan-Colás et al.

2.3 Interferometric Scattering Microscopy (iSCAT)

Interferometric Scattering Microscopy (iSCAT) is a single-molecule detection based approach. It relies on the light scattered by subwavelength objects. The signals come from the interference between the scattered light by the detected object and a reference light (**Figure 3d**). With the capability of single-molecule detection, iSCAT has shown its remarkably high sensitivity in cell imaging, single-particle tracking, label-free imaging of nanoscopic (dis)assembly, and quantitative single-molecule characterization [73]. Meanwhile, iSCAT microscopy itself does not provide adequate chemical or biological specificity due to its nature in collection of scattered light from all small objects [74].

McDonald et al. [75] reported an iSCAT contrast method to distinguish proteins secreted from an Epstein–Barr virus (EBV)-transformed B cell line (**Figure 3a**). The observed contrast on an iSCAT image reflects the amplitude of the electromagnetic field scattered by proteins, which is directedly correlated with the scattering cross-sections of detected molecules (**Figure 3c**). Here, the iSCAT demonstrated its capability of monitoring secreted proteins with varying molecular
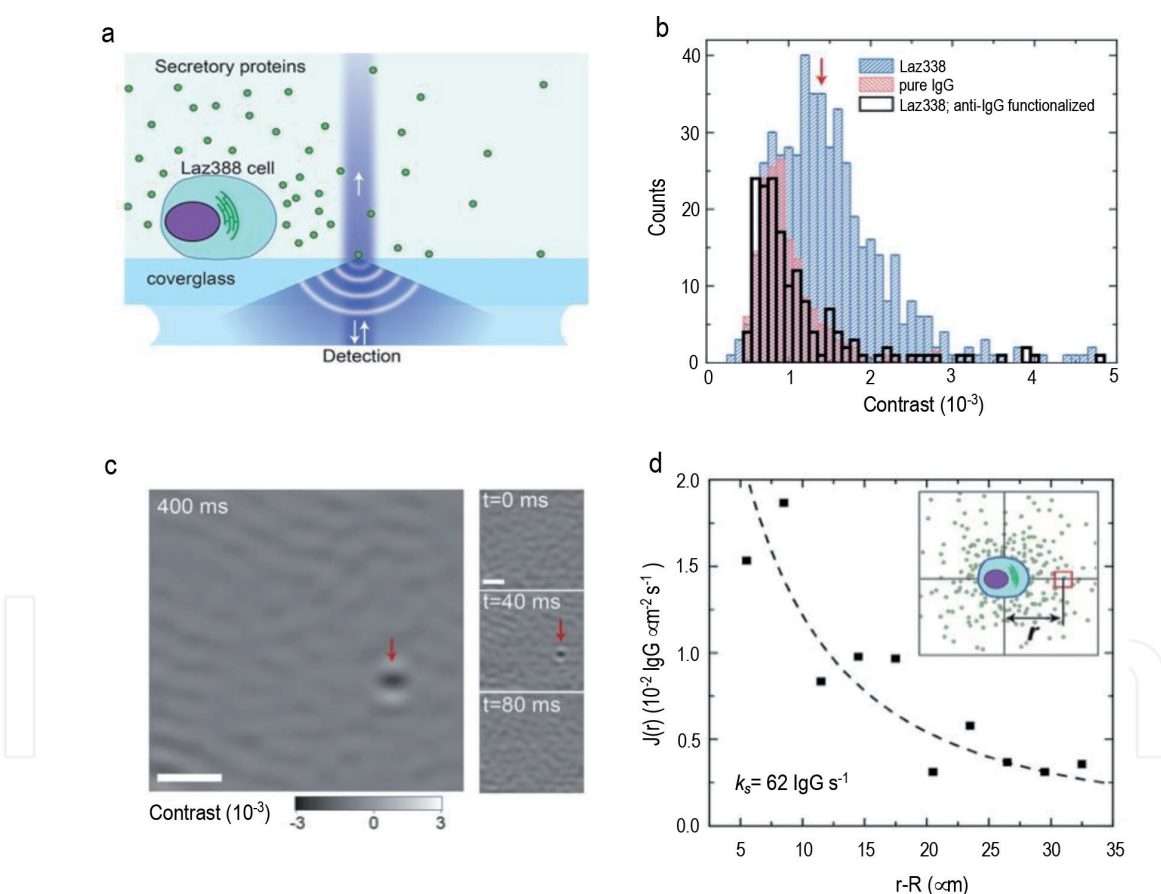

Figure 3.
Secretome quantification and identification. (a) Cartoon of the detection region. (b) Histogram of detected proteins during a 125 s long measurement period in which detected contrasts are counted in bins of 1×10^{-4} contrast (diagonal-hatched blue bars). 503 distinct proteins were counted in this period. The red arrow indicates the expected contrast corresponding to an IgG dimer. Superimposed over the cell secretion data is the contrast distribution of a purified IgG solution injected into the iSCAT FOV with a micropipette (diagonal-hatched rose bars, normalized for clarity). The detected secretion events from a single Laz388 cell on an anti-human IgG-functionalized coverglass are also shown (125 s integration, hollow black bars). The anti-human IgG surface selectively binds all four IgG antibody subtypes and resists the adsorption of other proteins. (c) Comparison of 2.5 fps (400 ms) and 25 fps (40 ms) image acquisitions of a single Laz388 cell's secretions. The right column shows three sequential 40 ms images, while the left displays the 400 ms image composed of 10 total images, including the three shown on the right. Scale bar: 1 μm. (d) IgG secretion rates and secretion heterogeneity. Reprinted (adapted) with permission from Ref. [28]. Copyright 2018 American Chemical Society.

weight 100 kDa–1 MDa. To provide iSCAT the detection specificity for human Immunoglobulin G(IgG), the sensing surface was functionalized with anti-human IgG, which showed high specificity on the adsorption event of IgG (**Figure 3b, d**). The quantification of IgG was realized by counting over certain integration period. It was found that the secretion of IgG antibodies in single Laz388 cells proceeded at a rate of 100 molecules per second.

One of the challenges in iSCAT for cell secretion is that, the recognition of small molecules is difficult due to their limited iSCAT contrast. In above work, the minimum protein molecular weight from iSCAT was approximately 100 kDa. Most cytokines have molecular weight range from approximately 6 to 70 kD, which fall out of the iSCAT's detection range.

3. Labelling techniques

3.1 Fluorescence

Fluorescence based detection provides superb sensitivity of detection, and flexibility in labeling. Fluorescence microscopy features high spatial and temporal resolution, and capability of tracking multiple cells simultaneously [14]. Therefore, fluorescence based detection has been widely used for tracking protein secretion.

3.1.1 FLUOROSpot

A simple and widely used method of single cell secretion analysis is the enzyme-linked immune absorbent spot (ELISpot) that utilizes the immunosandwich-based assay for the measurement of footprint of cells [76]. Cells are loaded into wells precoated with primary antibody. Secreted proteins are captured, and further bound with labeled secondary antibodies. The addition of substrate gives rise to the spots indicative of secretion footprint. Based on similar principle, FLUOROSpot was developed which uses fluorescent dyes to replace the enzyme labels. In this way, more than one protein could be analyzed at the same time [77]. In spite that ELISpot and FlUOROSpot have been used as common methods for the detection of cell secretion, several drawbacks hinder its applications in the real-time imaging of protein secretion, including spectral overlap, varied individual spots, limited temporal resolution caused by long incubation time (12–48 h), limited number of simultaneously tracked proteins, and cell lost during the process [78].

3.1.2 Microengraving

Inspired by the principle of FLUOROSpot, the microengraving method was developed to isolate and confine single cells in a planar array of microwells. The protein secretion of segregated cells can be tracked as protein detection microarrays are integrated with the microwells, which are conventionally made of elastomeric polymers such as polydimethylsiloxane (PDMS). These microfabricated wells have subnanoliter volumes. A glass side fabricated with antibodies is covered to the array of microwells, to capture the proteins secreted by confined cells. Subsequently, the slide is removed and incubated with fluorescently labelled secondary antibodies. The single-cell cytokine secretion analysis is implemented by fluorescence imaging. Bradshaw et al. [79] showed that the same cells in the microwell can be applied on two detection microarrays successively, allowing monitoring the secretion of four types of cytokines and antibodies. In the meantime, the segregated cells in the wells can also be directly stained by immunofluorescence to determine their lineages.

A drawback in this method is that, the tracked number of proteins is limited by the capability of differentiation of multiple fluorophores within a single spectrum.

3.1.3 Barcode chip

The number of secretion protein types from above methods is limited due to the spectral overlap as multiple fluorescence labels employed on the same detection chip. This spectral overlap was overcome by separating functionalized antibodies into different lines, using a barcode design. With a proper distance between, up to 15 parallel antibody lines can be contained within a nanoliter cell-trapping chamber. This improved spatial resolution results in an enhanced its capability of simultaneous multiplex detection [28, 29, 80]. Lu et al. [81] further extended the multiplexing capacity by further improving the spectral encoding, namely, in each isolated line, three antibodies with distinct fluorescent labels are contained. This strategy enables simultaneous analysis of 42 types of proteins secreted from a single cell.

Barcode chips provide valuable information for accumulated cell secretion over a period of time. However, the underlying limitations restrict its applications on the real-time monitoring of protein secretion. For instance, the lag between cell secretion and protein detection is inevitable since capture antibody and detection antibody have to play their part in distinct steps. Given their coexistence during cell secretion, strong background fluorescence signal is expected from the unbound labeled antibodies, thus secreted proteins are difficult to be distinguished from the background noise. In addition, to remove excess probes and avoid non-specific bindings, the sensor surface after incubation with cells requires intensive wash steps, which inhibits the shortening of analysis duration into a few hours.

3.1.4 Total internal reflection fluorescence microscopy (TIRFM)

Shiraskaki et al. [82] proposed a solution for the challenge mentioned above using total internal reflection fluorescence microscopy (TIRFM) combined with microengraving method. They deposited single cells on microwells, on the bottom of which anti-cytokine capture antibodies were fabricated. Instead of separate incubation of a sensor chip with a cell and the detection antibody, the fluorescent detection antibody is present in the cell culture medium, so the cytokine capture is in step with the binding of detection antibody. An objective lens of high numerical aperture was used to achieve high incidence angles, generating evanescence field. The near-field excitation by total internal refection enhances the fluorescence signal from the detection antibody in the sandwich immunocomplex, and reduces the background signal from the unbound detection antibodies in the culture medium (**Figure 4a**). With these features, imaging of cytokine secretion was achieved within a single step (**Figure 4b**). Meanwhile, the cell staining (calcein and SYTOX) was applied to investigate the membrane integrity during IL-1b secretion (**Figure 4c**). It was found the onset of IL-1b secretion was consistent with the onset of calcein disappearance and the second protein SYTOX influx (**Figure 4d**). This phenomenon indicated the loss of membrane during IL-1b secretion. The limit of detection of this approach reached down to 2000 cytokine molecules.

3.1.5 Nanoplasmonic fluorescence

The near-field excited fluorescence can also be realized by nanoplasmonic resonator. Wang et al. [83] developed a tunable nanoplasmonic resonator (TNPR) enhanced fluorescence immunoassay for imaging of IL-2 secretion in
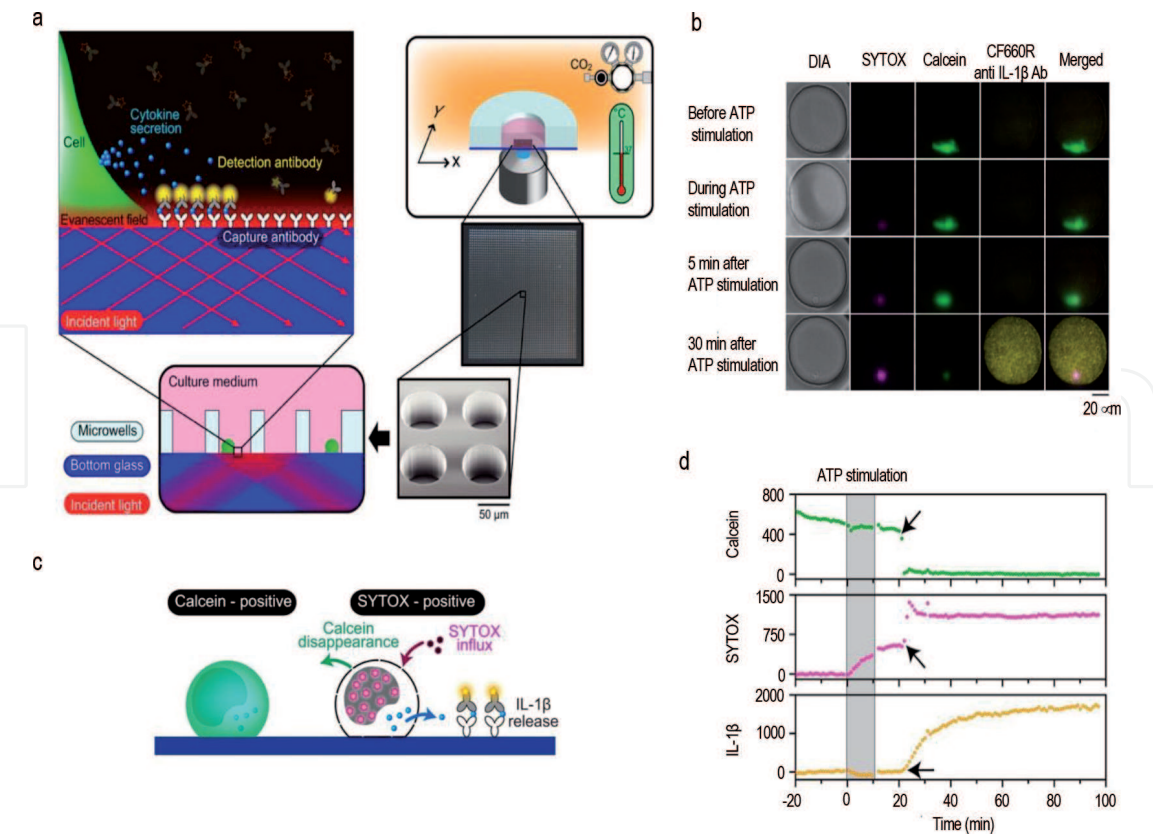
Figure 4.
Time-resolved monitoring of IL-1β secretion on the PDMS MWA chip. (a) Concept of the real-time single cell secretion assay platform. The platform works with micro-fabricated well-array chip on a fully automated fluorescence microscopy. The platform maintains the environment (temperature, concentration of CO_2 and humidity) of the chip. The chip has an array of nanolitre-sized microwells with a glass bottom, into which individual cells were introduced separately. The well has open-ended structure; therefore, culture medium was exchanged constantly during the observation. The anti-cytokine capture antibody was immobilized on the well bottom, onto which secreted cytokine and fluorescently labelled detection antibody were bound to form a sandwich immunocomplex. Near-field excitation by total internal reflection enabled selective detection of the cytokine sandwich immunocomplex immediately following secretion without the requirement for wash steps. (b) Representative images of multichannel microscopy. Morphological features of a human monocyte were monitored under diascopic illumination (DIA). The fluorescence signal of SYTOX-stained nuclei was magenta (SYTOX), that of a calcein-stained cell bodies was green (Calcein) and that of secreted IL-1β was yellow (CF660R anti IL-1β Ab). Merged images of these three fluorescence signals are also displayed (Merged). Each image was obtained at the described period. Scale bar, 20 μm. (c) Schematic of simultaneous monitoring of IL-1β secretion and cell membrane integrity using calcein and SYTOX staining. SYTOX influx and fluorescent calcein disappearance was observed due to compromised plasma membrane integrity. (d) Example of the signal time course during time-resolved monitoring. Grey bands represent the period when the monocytes were exposed to ATP. Arrows represent the transition time of the respective signals. Reprinted (adapted) with permission from Ref. [31]. Copyright 2014, Springer Nature.

submicrometer resolution (**Figure 5**). In this study, the fluorescent secondary antibody was not present while the cytokine secretion was in progress. Instead, cytokine capture and detection step was separated by washing step. With a TNPR structure of 100 nm in diameter, and an optimized fluorescence enhancement at ~10 nm from a gold surface, the fluorescence signal was enhanced 117-fold in the TNPR area. The limit of detection was lower than 100 ng/mL.

3.1.6 Bead biosensors

Another fluorescence based strategy is associated with bead-based biosensors. The cells are confined in microwells, along with antibody-labeled microbeads, and fluorescently-labeled secondary antibody. The capture of secreted proteins on beads was accompanied by the increasing density of secondary antibody, and increasing fluorescence intensity of microbeads. A key advantage of bead biosensors is that,
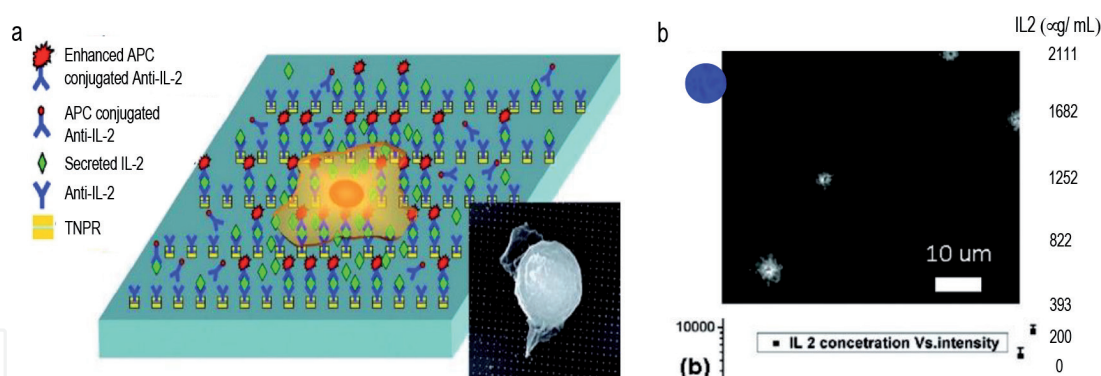
Figure 5.
Demonstration of quantitative high spatial resolution mapping of IL-2 secretion from individual Jurkat T cells. (a) Schematic of high-resolution mapping of cytokine secretion by a TNPR-enhanced in situ immunoassay. ATNPR array fabricated by NIL was incubated with anti-IL-2 antibody, and after Jurkat T cell plating, stimulation, and removal, a portion of the secreted IL-2 was captured by the antibodies on TNPR. Fluorescence-conjugated anti- bodies were applied to detect the secreted IL-2 by forming an antibody- antigen (IL-2)-antibody sandwich on the TNPR surface. Insert: SEM image of a Jurkat T cell adherent to a TNPR array (500 nm pitch). (b) quantitative mapping of Jurkat T cell secretion profiles. Reprinted (adapted) with permission from Ref. [50]. Copyright 2011 American Chemical Society.

it breaks the limit of target-molecular adsorption kinetics, which is controlled by diffusion rates, and exists in majority of immobilized or stationary biosensors [84]. In addition, the regeneration of biosensors can be as simple as removing used beads, and infusing new beads [85]. Son et al. [86] used microcompartments as small as 20 picoliter to confine single cells, suspended antibody-labeled microbeads, and fluorescently-labeled secondary antibody together. The quantitation of secreted cytokines was achieved by tracking the intensity changes of fluorescence on microbeads. They found that the number of microbeads confined within a single microcompartment did not significantly affect the fluorescence enhancement on a single microbead. An et al. [87] utilized a microwell device for cell confinement, and detected the fluorescence changes on functionalized detection beads which are co-incubated with single cells.

Other than the design of microwell, Cui et al. [88] developed an microfluidic immunoassay device that integrated a cell culture chamber, an array of cytokine detection units and an array of active peristaltic mixers for on-chip sample mixing. Cells were isolated, cultured and biochemically stimulated in the same chamber. The detection chambers were loaded with cytometric fluorescent beads. Upon sand-wich structure formed after cytokine secretion, the fluorescence intensity changes were analyzed by flow cytometry. The continuous monitoring of cytokine secre-tion was achieved by the extraction of a small portion of the cytokine-containing culture media to the detection chamber. With this system, the secretion profilings of IL-6, IL-8, and TNF were observed with a detection limit of 20 pg/mL and a sample volume of 160 nl.

3.1.7 Cell-surface affinity sensors

Cell-surface affinity sensors functionalize cell surface to capture secreted mol-ecules from cells. These targets can subsequently be detected by fluorescent labeling. An appealing advantage using this strategy is that, the effect of heterogeneous spatial distribution of secreted molecules is minimized [89, 90]. As secreted molecules release from the cell surface, their diffusion and dilution pose a challenge to the sensi-tivity of sensors. As the cell surface is turned into sensor surface, these molecules could be captured prior to their diffusion. This immediate interaction enhances the sensitivity of secretion detection. Various cell secretions have been studied previously

utilizing cell-surface affinity sensors, including ATP [91, 92], growth factors [93], cytokines [94], and antigens [95]. Liu et al. [96] developed a detection method that utilized fluorescent magnetic nanoparticles labeled secondary antibody, and achieved a detection limit of 0.1 pg/mL. The cell surface was biotinylated, and functionalized by neutravidin and a biotinylated IL-6 capture antibody. Upon the binding of cytokines secreted from cells, fluorescent magnetic nanoparticles labeled secondary antibodies are introduced for indication of the amount of cytokine secretion.

A challenge of cell-surface affinity sensors is the damage and cell viability caused by cell surface modification [97]. Due to the high background signal from free labeled secondary antibody, the cells after secretion have to undergo wash steps to remove free secondary antibodies. This limits its application on the real-time monitoring of cell secretion.

3.1.8 Droplet microfluidics

Droplet microfluidic techniques involve mixture of the aqueous phase and oil phase, and generation of water-in-oil microdroplets in the microfluidic chips [98]. Droplet shape offers encapsulation of a single cell in a picoliter droplet, which confines individual cell and entraps its secretion, restrains the interference from surrounding environment. To achieve real-time monitoring of cell secretion, droplets microfluidic techniques are conventionally integrated with cell-surface affinity sensors or bead-based biosensors. Qiu et al. [94] developed a membrane-anchored aptamer sensor and combined it with droplet microfluidics for IFN-γ detection. This aptamer sensor has a hairpin structure, resulting in quenched fluorescence. Upon binding with IFN-γ, the aptamer switches on the fluorescence signal by aptamer structure change. The limit of detection was approximately 10.0 nM. Due to the proximity of the aptamer sensor to the cell surface, this method achieved monitoring of cytokine secretion at a single-cell level. Chokkalingam et al. [99] took advantage of free capture beads in droplets to detect the secreted cytokines from cells. The cytokine capture step and fluorescent detection step were separated by the gelation of droplets, and de-emulsification. Wei et al. [100] combined LSPR with droplet technique, developing a sensor with a detection limit of 6–7 ng/ml for VEGF and IL-8. The LSPR spectrum shift was obtained by dark-field spectroscope. Due to the advantages of droplet technique, the plasmonic droplets in a continuous flow allow high-throughput detection of 600–1800 droplets/min, 100–150 cells/min.

4. Challenges and future trends

Isolated cell culture in a confined environment for subsequent secretion detection allows good flexibility in the selection of sensing techniques, but such module-based strategy has not been achieved for real-time detection of individual cell secretion. Meanwhile, the integration of cell culture and secretion detection has shown promising results in real-time monitoring single cell secretion by physically presenting the target cells in close proximity to the sensing region. However, there are still significant challenges and difficulties ahead as indicated below.

1. Cell secretion dynamics are found associated with cell states, therefore, it is important for the sensor systems to precisely quantify the cell secretion. An obstacle for current methodology is that, the molecule secretion and molecule detection are both dynamic process occurring at the same time.

The concentrations of target molecules in solution are constantly changing, such that an equilibrium-state based calibration curves are difficult to obtain. Therefore, on one hand, novel or improved detection methods with more rapidly reached equilibrium state are required to minimize the effect of detection process. On the other hand, a comprehensive dynamic model involving secretion and detection dynamics is necessary to understand this complex process and precisely quantify the cell secretion [101, 102].

2. The real-time imaging process requires highly specific and selective responses from sensors. Since the specificity and selectivity of biosensors might be compromised by non-specific binding in complex biological media used in experiments, significant efforts are needed to eliminate the matrix effect. Several blocking strategies that instantaneously passivate the sensor surface and do not affect the recognition chemistry are developed, including protein (like BSA), detergent (Tween, etc.), or different polymer blockers. In imaging experiments, a thoroughly optimized blocking strategy should be applied.

3. It is important to investigate the effects of important experiment conditions for the detection. Previous works mainly focused on the innovation of methodology, improvement of the sensitivity, enhancement of the capability of multiplex detection, etc. However, the influence of multiple important experimental conditions are lack of attention. For instance, in previous works, cells during their secretion were manipulated in various status, including suspended in media, immobilized on the ceiling of microwells, or directly absorbed on sensor surface. These distinct distances between sensing surface and cells are expected to influence the local concentrations of secretions on sensor surface, leading to considerate impact on detection sensitivity.

4. In current stage, multiplex real-time imaging of cell secretion is a great challenge. Though the fluorescence based barcode chip has demonstrated its capability in profiling up to 42 types of proteins secreted from a single cell, the real-time imaging of these proteins is incapable due to the lag between cell secretion and protein detection, and intensive wash steps which require several hours. Nanoplasmonic biosensors and SPR imaging have difficulty to broaden their multiplexity owing to their label-free characteristic. Therefore, to achieve the multiplex real-time imaging, the integration of these techniques might provide promising opportunities.

5. Current studies focus on the secretion of single type cells. The interactions of different cells, and their intercellular communication through proteins such as cytokines demand comprehension and further exploration. Therefore, a platform capable of monitoring of multiple cells' real-time secretion is demanded.

5. Conclusions

In the past two decades, cell secretion monitoring has gained increasing attention. To understand the heterogeneity of protein secretion in single cell level, various optic methods have been developed including labelling and label-free techniques. The label-free techniques such as plasmonic sensors, PCR, EOT, are able to recognize the secreted proteins by sensing the changes of refractive index on the sensor interfaces. The limit of detection differs from 20 pg/mL to 50 ng/mL. The signal transduction during the analyte-ligand interaction does not require

the involvement of any additional materials, therefore, the label-free techniques allow simple operation and fast response, suitable for real-time imaging. The labelling techniques such as fluorescence microscopy utilize fluorophore-labeled bioreceptors to recognize the proteins. Different from the label-free techniques, the fluorescence based methods conventionally use two recognition elements to form a sandwich complex, one of them as the capture element, the other as the signal transducer (the fluorophore-labeled bioreceptor). The limit of detection differs from 0.1 pg/mL to 20 ng/mL. Even though the two recognition element approaches involve additional processing and washing steps, which prolong the response time, the extraordinary sensitivity and low background improve the reliability and allow multiplex detection, making it very attractive to some applications.

For instance, TIRFM has demonstrated its possibilities on real-time imaging of protein secretion from single cells by utilizing both high sensitivity from fluorescence microscopy, and wash-free process due to the evanescent field created by total internal reflection. In spite of the achievements mentioned above, intensive work is demanded in future such as understanding of cell secretion dynamics, improving the detection specificity, developing multiplex real-time imaging platform, and investigating the interactions of different cells, and their intercellular communication.

Acknowledgements

Conflict of interest

The authors declare no conflict of interest.

Author details

Lang Zhou, Pengyu Chen and Aleksandr Simonian*
Materials Research and Education Center, Department of Mechanical Engineering, Auburn University, Auburn, AL 36849, USA

*Address all correspondence to: als@auburn.edu

IntechOpen

References

[1] Cavalli G, Cenci S. Autophagy and Protein Secretion. J Mol Biol [Internet]. 2020 Apr 3 [cited 2020 Sep 22];432(8):2525-45. Available from: https://www.sciencedirect.com/science/article/pii/S002228362030067X

[2] Uhlén M, Karlsson MJ, Hober A, Svensson A-S, Scheffel J, Kotol D, et al. The human secretome. Sci Signal [Internet]. 2019 Nov 26 [cited 2020 Sep 22];12(609). Available from: http://www.ncbi.nlm.nih.gov/pubmed/31772123

[3] Brandi J, Pozza ED, Dando I, Biondani G, Robotti E, Jenkins R, et al. Secretome protein signature of human pancreatic cancer stem-like cells. J Proteomics [Internet]. 2016 Mar 16 [cited 2020 Sep 22];136:1-12. Available from: https://www.sciencedirect.com/science/article/pii/S1874391916300203

[4] Baberg F, Geyh S, Waldera-Lupa D, Stefanski A, Zilkens C, Haas R, et al. Secretome analysis of human bone marrow derived mesenchymal stromal cells. Biochim Biophys Acta - Proteins Proteomics [Internet]. 2019 Apr 1 [cited 2020 Sep 22];1867(4):434-41. Available from: https://www.sciencedirect.com/science/article/pii/S1570963919300263

[5] Štrbák V. Pancreatic Thyrotropin Releasing Hormone and Mechanism of Insulin Secretion. Cell Physiol Biochem [Internet]. 2018 [cited 2020 Sep 22];50:378-84. Available from: www.karger.com/cpbwww.karger.com/cpb

[6] Ponpuak M, Mandell MA, Kimura T, Chauhan S, Cleyrat C, Deretic V. Secretory autophagy. Curr Opin Cell Biol [Internet]. 2015 Aug 1 [cited 2020 Sep 22];35:106-16. Available from: https://www.sciencedirect.com/science/article/pii/S0955067415000563

[7] Al-Qudah MA, Al-Dwairi A. Mechanisms and regulation of neurotrophin synthesis and secretion. Neurosciences (Riyadh) [Internet]. 2016 Oct [cited 2020 Sep 22];21(4):306-13. Available from: http://www.ncbi.nlm.nih.gov/pubmed/27744458

[8] Rabouille C. Pathways of Unconventional Protein Secretion. Trends Cell Biol [Internet]. 2017 Mar 1 [cited 2020 Sep 22];27(3):230-40. Available from: https://www.sciencedirect.com/science/article/pii/S0962892416302057

[9] Fujita-Yoshigaki J, Yokoyama M, Katsumata-Kato O. Determinants for selective transport of exogenously expressed cargo proteins into regulated and constitutive secretory pathways. J Oral Biosci [Internet]. 2017 May 1 [cited 2020 Sep 22];59(2):87-91. Available from: https://www.sciencedirect.com/science/article/pii/S1349007917300221?via%3Dihub

[10] Labunskyy VM, Gerashchenko M V., Delaney JR, Kaya A, Kennedy BK, Kaeberlein M, et al. Lifespan Extension Conferred by Endoplasmic Reticulum Secretory Pathway Deficiency Requires Induction of the Unfolded Protein Response. Kim SK, editor. PLoS Genet [Internet]. 2014 Jan 2 [cited 2020 Sep 22];10(1):e1004019. Available from: https://dx.plos.org/10.1371/journal.pgen.1004019

[11] Kienzle C, von Blume J. Secretory cargo sorting at the trans-Golgi network. Trends Cell Biol [Internet]. 2014 Oct 1 [cited 2020 Sep 22];24(10):584-93. Available from: https://www.sciencedirect.com/science/article/pii/S0962892414000725

[12] Ponnambalam S, Baldwin SA. Constitutive protein secretion from the trans -Golgi network to the plasma membrane (Review). Mol Membr Biol [Internet]. 2003 Jan 9 [cited 2020 Aug 22];20(2):129-39. Available from:

http://www.tandfonline.com/doi/full/1
0.1080/0968768031000084172

[13] Simpson JC, Joggerst B, Laketa V,
Verissimo F, Cetin C, Erfle H, et al.
Genome-wide RNAi screening identifies
human proteins with a regulatory
function in the early secretory pathway.
Nat Cell Biol [Internet]. 2012 Jul 3 [cited
2020 Aug 22];14(7):764-74. Available
from: http://www.nature.com/articles/
ncb2510

[14] Li W, Li D. Fluorescent probes
for monitoring regulated secretion.
Curr Opin Chem Biol [Internet]. 2013
Aug 1 [cited 2020 Aug 22];17(4):672-
81. Available from: https://www.
sciencedirect.com/science/article/pii/
S136759311300077X

[15] Meldolesi J. Exosomes and
Ectosomes in Intercellular
Communication. Curr Biol [Internet].
2018 Apr 23 [cited 2020 Sep
22];28(8):R435-44. Available from:
https://www.sciencedirect.com/science/
article/pii/S0960982218300927

[16] Diegeler S, Hellweg CE. Intercellular
Communication of Tumor Cells
and Immune Cells after Exposure to
Different Ionizing Radiation Qualities.
Front Immunol [Internet]. 2017 Jun 7
[cited 2020 Sep 22];8:664. Available
from: http://journal.frontiersin.org/
article/10.3389/fimmu.2017.00664/full

[17] Kveler K, Starosvetsky E, Ziv-
Kenet A, Kalugny Y, Gorelik Y,
Shalev-Malul G, et al. Immune-centric
network of cytokines and cells in disease
context identified by computational
mining of PubMed. Nat Biotechnol
[Internet]. 2018 Aug 18 [cited 2020 Sep
22];36(7):651-9. Available from: http://
www.nature.com/articles/nbt.4152

[18] Altan-Bonnet G, Mukherjee R.
Cytokine-mediated communication:
a quantitative appraisal of immune
complexity. Nat Rev Immunol
[Internet]. 2019 Apr 15 [cited 2020

Sep 22];19(4):205-17. Available from:
http://www.nature.com/articles/
s41577-019-0131-x

[19] Kulkarni A, Chen J, Maday S.
Neuronal autophagy and intercellular
regulation of homeostasis in the brain.
Curr Opin Neurobiol [Internet].
2018 Aug 1 [cited 2020 Sep 22];51:29-
36. Available from: https://www.
sciencedirect.com/science/article/pii/
S0959438818300011

[20] Kudryashova I V., Stepanichev MY,
Gulyaeva N V. Neonatal Proinflammatory
Stress and the Maturation of Intercellular
Communication in the Hippocampus.
Neurosci Behav Physiol [Internet]. 2020
Jul 5 [cited 2020 Sep 22];50(6):730-42.
Available from: http://link.springer.
com/10.1007/s11055-020-00971-6

[21] Osipova ED, Semyachkina-
Glushkovskaya O V., Morgun A V.,
Pisareva N V., Malinovskaya NA,
Boitsova EB, et al. Gliotransmitters
and cytokines in the control of
blood-brain barrier permeability.
Rev Neurosci [Internet]. 2018 Jul 26
[cited 2020 Sep 22];29(5):567-91.
Available from: http://www.degruyter.
com/view/j/revneuro.2018.29.
issue-5/revneuro-2017-0092/
revneuro-2017-0092.xml

[22] Patel BG, Lenk EE, Lebovic DI,
Shu Y, Yu J, Taylor RN. Pathogenesis
of endometriosis: Interaction between
Endocrine and inflammatory pathways.
Best Pract Res Clin Obstet Gynaecol
[Internet]. 2018 Jul 1 [cited 2020 Sep
22];50:50-60. Available from: https://
www.sciencedirect.com/science/article/
pii/S1521693418300233

[23] Tan C, Hu W, He Y, Zhang Y,
Zhang G, Xu Y, et al. Cytokine-
mediated therapeutic resistance in
breast cancer. Cytokine [Internet].
2018 Aug 1 [cited 2020 Sep 22];108:151-
9. Available from: https://www.
sciencedirect.com/science/article/pii/
S1043466618301066

[24] Esquivel-Velázquez M, Ostoa-Saloma P, Palacios-Arreola MI, Nava-Castro KE, Castro JI, Morales-Montor J. The Role of Cytokines in Breast Cancer Development and Progression. J Interf Cytokine Res [Internet]. 2015 Jan 13 [cited 2020 Sep 22];35(1):1-16. Available from: http://www.liebertpub.com/doi/10.1089/jir.2014.0026

[25] Balderman SR, Calvi LM. Biology of BM failure syndromes: role of microenvironment and niches. Hematology [Internet]. 2014 Dec 5 [cited 2020 Aug 22];2014(1):71-6. Available from: https://ashpublications.org/hematology/article/2014/1/71/20496/Biology-of-BM-failure-syndromes-role-of

[26] Clapes T, Lefkopoulos S, Trompouki E. Stress and Non-Stress Roles of Inflammatory Signals during HSC Emergence and Maintenance. Front Immunol [Internet]. 2016 Nov 7 [cited 2020 Aug 22];7:487. Available from: http://journal.frontiersin.org/article/10.3389/fimmu.2016.00487/full

[27] Cooper GM. The cell : a molecular approach [Internet]. ASM Press; 2000 [cited 2020 Aug 22]. 689 p. Available from: https://www.ncbi.nlm.nih.gov/books/NBK9839/

[28] Lu Y, Chen JJ, Mu L, Xue Q, Wu Y, Wu P-H, et al. High-Throughput Secretomic Analysis of Single Cells to Assess Functional Cellular Heterogeneity. Anal Chem [Internet]. 2013 Feb 19 [cited 2020 Aug 22];85(4):2548-56. Available from: https://pubs.acs.org/doi/10.1021/ac400082e

[29] Ma C, Fan R, Ahmad H, Shi Q, Comin-Anduix B, Chodon T, et al. A clinical microchip for evaluation of single immune cells reveals high functional heterogeneity in phenotypically similar T cells. Nat Med [Internet]. 2011 Jun 22 [cited 2020 Aug 22];17(6):738-43. Available from: http://www.nature.com/articles/nm.2375

[30] Deng Y, Zhang Y, Sun S, Wang Z, Wang M, Yu B, et al. An Integrated Microfluidic Chip System for Single-Cell Secretion Profiling of Rare Circulating Tumor Cells. Sci Rep [Internet]. 2015 May 16 [cited 2020 Aug 22];4(1):7499. Available from: http://www.nature.com/articles/srep07499

[31] Whiteside TL. The tumor microenvironment and its role in promoting tumor growth. Oncogene. 2008

[32] da Cunha BR, Domingos C, Buzzo Stefanini AC, Henrique T, Polachini GM, Castelo-Branco P, et al. Cellular interactions in the tumor microenvironment: The role of secretome. Journal of Cancer. 2019

[33] Liu W, Kin T, Ho S, Dorrell C, Campbell SR, Luo P, et al. Abnormal regulation of glucagon secretion by human islet alpha cells in the absence of beta cells. EBioMedicine [Internet]. 2019 Dec 1 [cited 2020 Aug 22];50:306-16. Available from: https://www.sciencedirect.com/science/article/pii/S2352396419307674

[34] Del Prato S, Bianchi C, Daniele G. Abnormalities of Insulin Secretion and β-Cell Defects in Type 2 Diabetes. In: Textbook of Diabetes [Internet]. Chichester, UK: John Wiley & Sons, Ltd; 2016 [cited 2020 Aug 22]. p. 161-73. Available from: http://doi.wiley.com/10.1002/9781118924853.ch12

[35] Showalter A, Limaye A, Oyer JL, Igarashi R, Kittipatarin C, Copik AJ, et al. Cytokines in immunogenic cell death: Applications for cancer immunotherapy. Cytokine [Internet]. 2017 Sep 1 [cited 2020 Aug 22];97:123-32. Available from: https://www.sciencedirect.com/science/article/pii/S1043466617301539

[36] Tong L, Wei H, Zhang S, Xu H. Recent Advances in Plasmonic Sensors. Sensors [Internet]. 2014 May

5 [cited 2020 Sep 22];14(5):7959-73. Available from: http://www.mdpi.com/1424-8220/14/5/7959

[37] Kazanskiy NL, Khonina SN, Butt MA. Plasmonic sensors based on Metal-insulator-metal waveguides for refractive index sensing applications: A brief review. Phys E Low-dimensional Syst Nanostructures [Internet]. 2020 Mar 1 [cited 2020 Sep 22];117:113798. Available from: https://www.sciencedirect.com/science/article/pii/S1386947719311336

[38] Barizuddin S, Bok S, Gangopadhyay S. Plasmonic Sensors for Disease Detection - A Review. J Nanomed Nanotechnol [Internet]. 2016 [cited 2020 Sep 22];7:373. Available from: http://dx.doi.org/10.4172/2157-7439.1000373

[39] Sharma AK, Pandey AK, Kaur B. A Review of advancements (2007-2017) in plasmonics-based optical fiber sensors. Opt Fiber Technol [Internet]. 2018 Jul 1 [cited 2020 Sep 22];43:20-34. Available from: https://www.sciencedirect.com/science/article/pii/S1068520018300324

[40] Jeon TY, Kim DJ, Park S-G, Kim S-H, Kim D-H. Nanostructured plasmonic substrates for use as SERS sensors. Nano Converg [Internet]. 2016 Dec 1 [cited 2020 Sep 22];3(1):18. Available from: http://nanoconvergencejournal.springeropen.com/articles/10.1186/s40580-016-0078-6

[41] Wang J, Lin W, Cao E, Xu X, Liang W, Zhang X. Surface Plasmon Resonance Sensors on Raman and Fluorescence Spectroscopy. Sensors [Internet]. 2017 Nov 24 [cited 2020 Sep 22];17(12):2719. Available from: http://www.mdpi.com/1424-8220/17/12/2719

[42] Wang D-S, Fan S-K. Microfluidic Surface Plasmon Resonance Sensors: From Principles to Point-of-Care Applications. Sensors [Internet]. 2016 Jul 27 [cited 2020 Sep 22];16(8):1175. Available from: http://www.mdpi.com/1424-8220/16/8/1175

[43] Jackman JA, Yorulmaz Avsar S, Ferhan AR, Li D, Park JH, Zhdanov VP, et al. Quantitative Profiling of Nanoscale Liposome Deformation by a Localized Surface Plasmon Resonance Sensor. Anal Chem [Internet]. 2017 Jan 17 [cited 2020 Sep 22];89(2):1102-9. Available from: https://pubs.acs.org/doi/10.1021/acs.analchem.6b02532

[44] Kim H-M, Park J-H, Jeong DH, Lee H-Y, Lee S-K. Real-time detection of prostate-specific antigens using a highly reliable fiber-optic localized surface plasmon resonance sensor combined with micro fluidic channel. Sensors Actuators B Chem [Internet]. 2018 Nov 10 [cited 2020 Sep 22];273:891-8. Available from: https://www.sciencedirect.com/science/article/pii/S0925400518312449

[45] Blanchard-Dionne A-P, Meunier M. Sensing with periodic nanohole arrays. Adv Opt Photonics [Internet]. 2017 Dec 31 [cited 2020 Sep 22];9(4):891. Available from: https://www.osapublishing.org/abstract.cfm?URI=aop-9-4-891

[46] Jackman JA, Linardy E, Yoo D, Seo J, Ng WB, Klemme DJ, et al. Plasmonic Nanohole Sensor for Capturing Single Virus-Like Particles toward Virucidal Drug Evaluation. Small [Internet]. 2016 Mar 1 [cited 2020 Sep 22];12(9):1159-66. Available from: http://doi.wiley.com/10.1002/smll.201501914

[47] Schasfoort R, Abali F, Stojanovic I, Vidarsson G, Terstappen L. Trends in SPR Cytometry: Advances in Label-Free Detection of Cell Parameters. Biosensors [Internet]. 2018 Oct 30 [cited 2020 Aug 22];8(4):102. Available from: http://www.mdpi.com/2079-6374/8/4/102

[48] Liu C, Lei T, Ino K, Matsue T, Tao N, Li C-Z. Real-time monitoring biomarker expression of carcinoma

cells by surface plasmon resonance biosensors. Chem Commun [Internet]. 2012 Sep 26 [cited 2020 Aug 20];48(84):10389. Available from: http://xlink.rsc.org/?DOI=2cc34853e

[49] Milgram S, Cortes S, Villiers MB, Marche P, Buhot A, Livache T, et al. On chip real time monitoring of B-cells hybridoma secretion of immunoglobulin. Biosens Bioelectron. 2011 Jan 15;**26**(5):2728-2732

[50] Wu C, He J, Li B, Xu Y, Gu D, Liu H, et al. Real-time monitoring of T-cell-secreted interferon-γ for the diagnosis of tuberculosis. Biotechnol Biotechnol Equip [Internet]. 2018 Jul 4 [cited 2020 Mar 2];32(4):993-8. Available from: https://www.tandfonline.com/doi/full/10.1080/13102818.2018.1432416

[51] Stojanović I, van der Velden TJG, Mulder HW, Schasfoort RBM, Terstappen LWMM. Quantification of antibody production of individual hybridoma cells by surface plasmon resonance imaging. Anal Biochem [Internet]. 2015 Sep 15 [cited 2020 Aug 20];485:112-8. Available from: https://www.sciencedirect.com/science/article/pii/S0003269715003115

[52] Stojanović I, Baumgartner W, van der Velden TJG, Terstappen LWMM, Schasfoort RBM. Modeling single cell antibody excretion on a biosensor. Anal Biochem [Internet]. 2016 Jul 1 [cited 2020 Aug 20];504:1-3. Available from: https://www.sciencedirect.com/science/article/pii/S0003269716300094

[53] Puiu M, Bala C. SPR and SPR Imaging: Recent Trends in Developing Nanodevices for Detection and Real-Time Monitoring of Biomolecular Events. Sensors [Internet]. 2016 Jun 14 [cited 2020 Aug 22];16(6):870. Available from: http://www.mdpi.com/1424-8220/16/6/870

[54] Homola J. Surface Plasmon Resonance Sensors for Detection of Chemical and Biological Species. 2008 [cited 2020 Aug 22]; Available from: https://pubs.acs.org/doi/full/10.1021/cr068107d

[55] Spoto G, Minunni M. Surface Plasmon Resonance Imaging: What Next? J Phys Chem Lett [Internet]. 2012 Sep 20 [cited 2020 Aug 22];3(18):2682-91. Available from: https://pubs.acs.org/doi/10.1021/jz301053n

[56] Wang D, Loo J, Chen J, Yam Y, Chen S-C, He H, et al. Recent Advances in Surface Plasmon Resonance Imaging Sensors. Sensors [Internet]. 2019 Mar 13 [cited 2020 Aug 22];19(6):1266. Available from: https://www.mdpi.com/1424-8220/19/6/1266

[57] Bryce P. Nelson, Anthony G. Frutos, Jennifer M. Brockman and, Corn* RM. Near-Infrared Surface Plasmon Resonance Measurements of Ultrathin Films. 1. Angle Shift and SPR Imaging Experiments. 1999 [cited 2020 Aug 22]; Available from: https://pubs.acs.org/doi/abs/10.1021/ac990517x

[58] Mukherji S, Shukla G. Nanoplasmonic biosensors: current perspectives. Nanobiosensors Dis Diagnosis [Internet]. 2015 Sep 10 [cited 2020 Aug 22];4:75. Available from: https://www.dovepress.com/nanoplasmonic-biosensors-current-perspectives-peer-reviewed-article-NDD

[59] Mazzotta F, Johnson TW, Dahlin AB, Shaver J, Oh S-H, Höök F. Influence of the Evanescent Field Decay Length on the Sensitivity of Plasmonic Nanodisks and Nanoholes. ACS Photonics [Internet]. 2015 Feb 18 [cited 2020 Aug 22];2(2):256-62. Available from: https://pubs.acs.org/doi/10.1021/ph500360d

[60] Peixoto de Almeida M, Pereira E, Baptista P, Gomes I, Figueiredo S, Soares L, et al. Gold Nanoparticles as (Bio)Chemical Sensors. Compr Anal

Chem [Internet]. 2014 Jan 1 [cited 2020 Aug 22];66:529-67. Available from: https://www.sciencedirect.com/science/article/pii/B9780444632852000134

[61] Jackman JA, Rahim Ferhan A, Cho N-J. Nanoplasmonic sensors for biointerfacial science. Chem Soc Rev [Internet]. 2017 Jun 19 [cited 2020 Aug 22];46(12):3615-60. Available from: http://xlink.rsc.org/?DOI=C6CS00494F

[62] Zhu C, Luo X, Espulgar WV, Koyama S, Kumanogoh A, Saito M, et al. Real-Time Monitoring and Detection of Single-Cell Level Cytokine Secretion Using LSPR Technology. Micromachines [Internet]. 2020 Jan 19 [cited 2020 Feb 19];11(1):107. Available from: https://www.mdpi.com/2072-666X/11/1/107

[63] Oh B-R, Chen P, Nidetz R, McHugh W, Fu J, Shanley TP, et al. Multiplexed Nanoplasmonic Temporal Profiling of T-Cell Response under Immunomodulatory Agent Exposure. ACS Sensors [Internet]. 2016 Jul 22 [cited 2020 Aug 20];1(7):941-8. Available from: https://pubs.acs.org/doi/10.1021/acssensors.6b00240

[64] Faridi A, Yang W, Kelly HG, Wang C, Faridi P, Purcell AW, et al. Differential Roles of Plasma Protein Corona on Immune Cell Association and Cytokine Secretion of Oligomeric and Fibrillar Beta-Amyloid. Biomacromolecules [Internet]. 2019 Nov 11 [cited 2020 Aug 20];20(11):4208-17. Available from: https://pubs.acs.org/doi/10.1021/acs.biomac.9b01116

[65] Ahmad Mohamed Ali R, Mita D, Espulgar W, Saito M, Nishide M, Takamatsu H, et al. Single Cell Analysis of Neutrophils NETs by Microscopic LSPR Imaging System. Micromachines [Internet]. 2019 Dec 31 [cited 2020 Aug 20];11(1):52. Available from: https://www.mdpi.com/2072-666X/11/1/52

[66] Raphael MP, Christodoulides JA, Delehanty JB, Long JP, Byers JM. Quantitative Imaging of Protein Secretions from Single Cells in Real Time. Biophys J [Internet]. 2013 Aug 6 [cited 2020 Aug 20];105(3):602-8. Available from: https://www.sciencedirect.com/science/article/pii/S0006349513007017

[67] Escobedo C, Brolo AG, Gordon R, Sinton D. Flow-Through vs Flow-Over: Analysis of Transport and Binding in Nanohole Array Plasmonic Biosensors. Anal Chem [Internet]. 2010 Dec 15 [cited 2020 Aug 22];82(24):10015-20. Available from: https://pubs.acs.org/doi/10.1021/ac101654f

[68] Li X, Soler M, Özdemir CI, Belushkin A, Yesilköy F, Altug H. Plasmonic nanohole array biosensor for label-free and real-time analysis of live cell secretion. Lab Chip. 2017 Jun 27;**17**(13):2208-2217

[69] Li X, Soler M, Szydzik C, Khoshmanesh K, Schmidt J, Coukos G, et al. Label-Free Optofluidic Nanobiosensor Enables Real-Time Analysis of Single-Cell Cytokine Secretion. Small [Internet]. 2018 Jun 27 [cited 2020 Feb 20];14(26):1800698. Available from: http://doi.wiley.com/10.1002/smll.201800698

[70] Pitruzzello G, Krauss TF. Photonic crystal resonances for sensing and imaging. J Opt [Internet]. 2018 Jul 1 [cited 2020 Aug 22];20(7):073004. Available from: https://iopscience.iop.org/article/10.1088/2040-8986/aac75b

[71] Triggs GJ, Fischer M, Stellinga D, Scullion MG, Evans GJO, Krauss TF. Spatial Resolution and Refractive Index Contrast of Resonant Photonic Crystal Surfaces for Biosensing. IEEE Photonics J [Internet]. 2015 Jun [cited 2020 Aug 22];7(3):1-10. Available from: http://ieeexplore.ieee.org/document/7110507/

[72] Juan-Colás J, Hitchcock IS, Coles M, Johnson S, Krauss TF. Quantifying

single-cell secretion in real time using resonant hyperspectral imaging. Proc Natl Acad Sci U S A. 2018 Dec 26;**115**(52):13204-13209

[73] Young G, Kukura P. Interferometric Scattering Microscopy. Annu Rev Phys Chem [Internet]. 2019 Jun 14 [cited 2020 Aug 22];70(1):301-22. Available from: https://www.annualreviews.org/doi/10.1146/annurev-physchem-050317-021247

[74] Park J-S, Lee I-B, Moon H-M, Joo J-H, Kim K-H, Hong S-C, et al. Label-free and live cell imaging by interferometric scattering microscopy. Chem Sci [Internet]. 2018 Mar 7 [cited 2020 Aug 22];9(10):2690-7. Available from: http://xlink.rsc.org/?DOI=C7SC04733A

[75] McDonald MP, Gemeinhardt A, König K, Piliarik M, Schaffer S, Völkl S, et al. Visualizing Single-Cell Secretion Dynamics with Single-Protein Sensitivity. Nano Lett. 2018 Jan 10;**18**(1):513-519

[76] Crotty S, Aubert RD, Glidewell J, Ahmed R. Tracking human antigen-specific memory B cells: a sensitive and generalized ELISPOT system. J Immunol Methods [Internet]. 2004 Mar 1 [cited 2020 Aug 21];286(1-2):111-22. Available from: https://www.sciencedirect.com/science/article/pii/S0022175904000031

[77] Janetzki S, Rueger M, Dillenbeck T. Stepping up ELISpot: Multi-Level Analysis in FluoroSpot Assays. Cells [Internet]. 2014 Nov 27 [cited 2020 Aug 22];3(4):1102-15. Available from: http://www.mdpi.com/2073-4409/3/4/1102

[78] Han Q, Bradshaw EM, Nilsson B, Hafler DA, Love JC. Multidimensional analysis of the frequencies and rates of cytokine secretion from single cells by quantitative microengraving. Lab Chip [Internet]. 2010 May 18 [cited 2020 Aug 22];10(11):1391. Available from: http://xlink.rsc.org/?DOI=b926849a

[79] Bradshaw EM, Kent SC, Tripuraneni V, Orban T, Ploegh HL, Hafler DA, et al. Concurrent detection of secreted products from human lymphocytes by microengraving: Cytokines and antigen-reactive antibodies. Clin Immunol [Internet]. 2008 Oct 1 [cited 2020 Aug 21];129(1):10-8. Available from: https://www.sciencedirect.com/science/article/pii/S1521661608006888

[80] Fan R, Vermesh O, Srivastava A, Yen BKH, Qin L, Ahmad H, et al. Integrated barcode chips for rapid, multiplexed analysis of proteins in microliter quantities of blood. Nat Biotechnol [Internet]. 2008 Dec 16 [cited 2020 Aug 22];26(12):1373-8. Available from: http://www.nature.com/articles/nbt.1507

[81] Lu Y, Xue Q, Eisele MR, Sulistijo ES, Brower K, Han L, et al. Highly multiplexed profiling of single-cell effector functions reveals deep functional heterogeneity in response to pathogenic ligands. Proc Natl Acad Sci U S A [Internet]. 2015 Feb 17 [cited 2020 Aug 21];112(7):E607-15. Available from: http://www.ncbi.nlm.nih.gov/pubmed/25646488

[82] Shirasaki Y, Yamagishi M, Suzuki N, Izawa K, Nakahara A, Mizuno J, et al. Real-time single-cell imaging of protein secretion. Sci Rep [Internet]. 2015 May 22 [cited 2020 Aug 22];4(1):4736. Available from: http://www.nature.com/articles/srep04736

[83] Wang S, Ota S, Guo B, Ryu J, Rhodes C, Xiong Y, et al. Subcellular resolution mapping of endogenous cytokine secretion by nano-plasmonic-resonator sensor array. Nano Lett. 2011 Aug 10;**11**(8):3431-3434

[84] Cohen N, Sabhachandani P, Golberg A, Konry T. Approaching near real-time biosensing: Microfluidic microsphere based biosensor for real-time analyte detection. Biosens

Bioelectron [Internet]. 2015 Apr 15 [cited 2020 Aug 22];66:454-60. Available from: https://www.sciencedirect.com/science/article/pii/S0956566314009075

[85] Son KJ, Gheibi P, Stybayeva G, Rahimian A, Revzin A. Detecting cell-secreted growth factors in microfluidic devices using bead-based biosensors. Microsystems Nanoeng [Internet]. 2017 Dec 3 [cited 2020 Aug 22];3(1):17025. Available from: http://www.nature.com/articles/micronano201725

[86] Son KJ, Rahimian A, Shin D-S, Siltanen C, Patel T, Revzin A. Microfluidic compartments with sensing microbeads for dynamic monitoring of cytokine and exosome release from single cells. Analyst [Internet]. 2016 Jan 4 [cited 2020 Aug 22];141(2):679-88. Available from: http://xlink.rsc.org/?DOI=C5AN01648G

[87] An X, Sendra VG, Liadi I, Ramesh B, Romain G, Haymaker C, et al. Single-cell profiling of dynamic cytokine secretion and the phenotype of immune cells. Ahlenstiel G, editor. PLoS One [Internet]. 2017 Aug 24 [cited 2020 Aug 22];12(8):e0181904. Available from: https://dx.plos.org/10.1371/journal.pone.0181904

[88] Cui X, Liu Y, Hu D, Qian W, Tin C, Sun D, et al. A fluorescent microbead-based microfluidic immunoassay chip for immune cell cytokine secretion quantification. Lab Chip. 2018 Jan 30;**18**(3):522-531

[89] Wimmers F, Subedi N, van Buuringen N, Heister D, Vivié J, Beeren-Reinieren I, et al. Single-cell analysis reveals that stochasticity and paracrine signaling control interferon-alpha production by plasmacytoid dendritic cells. Nat Commun [Internet]. 2018 Dec 20 [cited 2020 Aug 22];9(1):3317. Available from: http://www.nature.com/articles/s41467-018-05784-3

[90] Qiu L, Zhang T, Jiang J, Wu C, Zhu G, You M, et al. Cell Membrane-Anchored Biosensors for Real-Time Monitoring of the Cellular Microenvironment. J Am Chem Soc [Internet]. 2014 Sep 24 [cited 2020 Aug 22];136(38):13090-3. Available from: https://pubs.acs.org/doi/10.1021/ja5047389

[91] Lobas MA, Tao R, Nagai J, Kronschläger MT, Borden PM, Marvin JS, et al. A genetically encoded single-wavelength sensor for imaging cytosolic and cell surface ATP. Nat Commun [Internet]. 2019 Dec 12 [cited 2020 Aug 22];10(1):711. Available from: http://www.nature.com/articles/s41467-019-08441-5

[92] Beigi R, Kobatake E, Aizawa M, Dubyak GR. Detection of local ATP release from activated platelets using cell surface-attached firefly luciferase. https://doi.org/101152/ajpcell19992761C267 [Internet]. 1999 [cited 2020 Aug 22]; Available from: https://journals.physiology.org/doi/full/10.1152/ajpcell.1999.276.1.C267

[93] Zhao W, Schafer S, Choi J, Yamanaka YJ, Lombardi ML, Bose S, et al. Cell-surface sensors for real-time probing of cellular environments. Nat Nanotechnol [Internet]. 2011 Aug 17 [cited 2020 Aug 22];6(8):524-31. Available from: http://www.nature.com/articles/nnano.2011.101

[94] Qiu L, Wimmers F, Weiden J, Heus HA, Tel J, Figdor CG. A membrane-anchored aptamer sensor for probing IFNγ secretion by single cells. Chem Commun [Internet]. 2017 Jul 13 [cited 2020 Aug 22];53(57):8066-9. Available from: http://xlink.rsc.org/?DOI=C7CC03576D

[95] Zhang J, Jin R, Jiang D, Chen H-Y. Electrochemiluminescence-Based Capacitance Microscopy for Label-Free Imaging of Antigens on the Cellular Plasma Membrane. J Am Chem Soc

[Internet]. 2019 Jul 3 [cited 2020 Aug 22];141(26):10294-9. Available from: https://pubs.acs.org/doi/10.1021/jacs.9b03007

[96] Liu G, Bursill C, Cartland SP, Anwer AG, Parker LM, Zhang K, et al. A Nanoparticle-Based Affinity Sensor that Identifies and Selects Highly Cytokine-Secreting Cells. iScience [Internet]. 2019 Oct 25 [cited 2020 Aug 22];20:137-47. Available from: https://www.sciencedirect.com/science/article/pii/S2589004219303578?via%3Dihub

[97] Hernandez-Fuentes MP, Warrens AN, Lechler RI. Immunologic monitoring. Immunol Rev [Internet]. 2003 Dec 1 [cited 2020 Aug 22];196(1):247-64. Available from: http://doi.wiley.com/10.1046/j.1600-065X.2003.00092.x

[98] Rotem A, Ram O, Shoresh N, Sperling RA, Goren A, Weitz DA, et al. Single-cell ChIP-seq reveals cell subpopulations defined by chromatin state. Nat Biotechnol [Internet]. 2015 Nov 12 [cited 2020 Aug 22];33(11):1165-72. Available from: http://www.nature.com/articles/nbt.3383

[99] Chokkalingam V, Tel J, Wimmers F, Liu X, Semenov S, Thiele J, et al. Probing cellular heterogeneity in cytokine-secreting immune cells using droplet-based microfluidics. Lab Chip [Internet]. 2013 Nov 12 [cited 2020 Aug 22];13(24):4740. Available from: http://xlink.rsc.org/?DOI=c3lc50945a

[100] Wei S-C, Hsu MN, Chen C-H. Plasmonic droplet screen for single-cell secretion analysis. Biosens Bioelectron [Internet]. 2019 Nov 1 [cited 2020 Aug 22];144:111639. Available from: https://www.sciencedirect.com/science/article/pii/S0956566319307183

[101] Stephens DC, Osunsanmi N, Sochacki KA, Powell TW, Taraska JW, Harris DA. Spatiotemporal organization and protein dynamics involved in regulated exocytosis of MMP-9 in breast cancer cells. J Gen Physiol [Internet]. 2019 Dec 2 [cited 2020 Aug 22];151(12):1386-403. Available from: https://rupress.org/jgp/article/151/12/1386/132562/Spatiotemporal-organization-and-protein-dynamics

[102] Chen Z, Lu Y, Zhang K, Xiao Y, Lu J, Fan R. Multiplexed, Sequential Secretion Analysis of the Same Single Cells Reveals Distinct Effector Response Dynamics Dependent on the Initial Basal State. Adv Sci [Internet]. 2019 May 13 [cited 2020 Aug 22];6(9):1801361. Available from: https://onlinelibrary.wiley.com/doi/abs/10.1002/advs.201801361